OXFORD

Prophylactic Administration of Mesenchymal Stromal Cells Does Not Prevent Arrested Lung Development in Extremely Premature-Born Non-Human Primates

Marius A. Möbius[1,2,3,4,] , **Steven R. Seidner**[4,] , **Donald C. McCurnin**[4], **Leonhard Menschner**[1,2,] ,
Isabel Fürböter-Behnert[1,2], **Julia Schönfeld**[1,2,] , **Jenny Marzahn**[1,2], **Daniel Freund**[1,3,] ,
Nadine Münch[1,3], **Sandra Hering**[5], **Shamimunisa B. Mustafa**[4], **Diana G. Anzueto**[4],
Lauryn A. Winter[4], **Cynthia L. Blanco**[4], **Martha A. Hanes**[6], **Mario Rüdiger**[1,2,‡,] ,
Bernard Thébaud[*,7,8,9,‡,]

[1]Neonatology and Pediatric Critical Care Medicine, Department of Pediatrics, University Hospital Carl Gustav Carus, Technische Universität Dresden, Dresden, Saxony, Germany
[2]Saxonian Center for Feto/ Neonatal Health, Medical Faculty Carl Gustav Carus, Technische Universität Dresden, Dresden, Saxony, Germany
[3]Good Manufacturing Practice, Center for Regenerative Therapies, Technische Universität Dresden, Dresden, Saxony, Germany
[4]Neonatology, Department of Pediatrics, University of Texas Health Science Center at San Antonio, San Antonio, TX, USA
[5]Forensic Genetics, Institute for Legal Medicine, Medical Faculty Carl Gustav Carus, Technische Universität Dresden, Dresden, Saxony, Germany
[6]Pathology Services, Laboratory Animal Resources, University of Texas Health Science Center at San Antonio, San Antonio, TX, USA
[7]Regenerative Medicine Program, Ottawa Hospital Research Institute, Ottawa, ON, Canada
[8]Neonatology, Department of Pediatrics, Children's Hospital of Eastern Ontario (CHEO) and CHEO Research Institute, Ottawa, ON, Canada
[9]Department of Cellular and Molecular Medicine, University of Ottawa, Ottawa, ON, Canada
*Corresponding author: Bernard Thébaud, MD, PhD, The Ottawa Hospital Research Institute, 501 Smyth Road, Ottawa, ON, Canada K1H 8L6. Tel: +1 613 737 8899; E-mail: bthebaud@ohri.ca
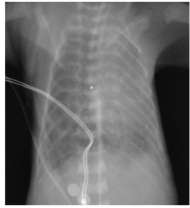‡Contributed equally.

Abstract

Premature birth is a leading cause of childhood morbidity and mortality and often followed by an arrest of postnatal lung development called bronchopulmonary dysplasia. Therapies using exogenous mesenchymal stromal cells (MSC) have proven highly efficacious in term-born rodent models of this disease, but effects of MSC in actual premature-born lungs are largely unknown. Here, we investigated thirteen non-human primates (baboons; *Papio* spp.) that were born at the limit of viability and given a single, intravenous dose of ten million human umbilical cord tissue-derived MSC per kilogram or placebo immediately after birth. Following two weeks of human-equivalent neonatal intensive care including mechanical ventilation, lung function testing and echocardiographic studies, lung tissues were analyzed using unbiased stereology. We noted that therapy with MSC was feasible, safe and without signs of engraftment when administered as controlled infusion over 15 minutes, but linked to adverse events when given faster. Administration of cells was associated with improved cardiovascular stability, but neither benefited lung structure, nor lung function after two weeks of extrauterine life. We concluded that a single, intravenous administration of MSC had no short- to mid-term lung-protective effects in extremely premature-born baboons, sharply contrasting data from term-born rodent models of arrested post-natal lung development and urging for investigations on the mechanisms of cell-based therapies for diseases of prematurity in actual premature organisms.

Key words: bronchopulmonary dysplasia; lung development; extreme premature birth; cell therapy; adverse events; unbiased stereology.
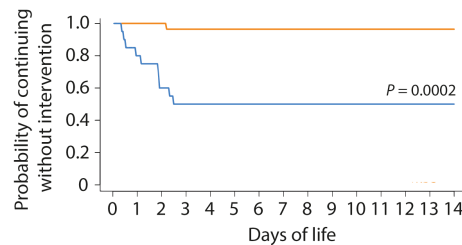
Graphical Abstract

Extremely preterm-born baboons received **UC-MSC** or **Placebo** immediately after birth → 14 days human-equivalent neonatal intensive care therapy including invasive ventilation → Physiological data analysis Functional structure preservation Morphometry by stereology

UC-MSC are safe, but prompt severe adverse events when injected too fast

UC-MSC improve cardiovascular stability and reduce inotrope demand versus Placebo
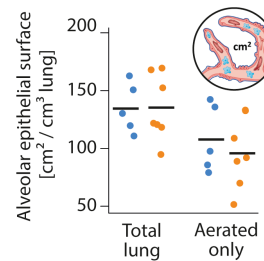
No impact of UC-MSC on lung structure or function

Significance Statement

Therapies using mesenchymal stem- or stromal cells (MSC) gained unprecedented attention as intervention for bronchopulmonary dysplasia (BPD), a common and incurable lung disease characterized by arrested pulmonary development after being born too early ("premature"). Using unbiased morphometric analysis methods, we here demonstrate that MSC—albeit being highly efficacious in term-born rodent models of BPD—do not benefit arrested lung development in extremely premature-born, ventilated baboons receiving 2 weeks of human-equivalent neonatal intensive care. Our research suggests fundamentally different mechanisms of MSC action in extremely premature and term-born lungs, warranting further investigations.

Introduction

Prematurity—i.e., birth before completing 37 weeks of gestation—and its complications account for the highest number of deaths in children below the age of 5 years.[1] The chronic lung disease bronchopulmonary dysplasia (BPD) is the most common complication of prematurity, characterized by postnatal impairment of alveolarization (failure to increase the surface area available for gas exchange by formation of secondary alveolar septa) and vascularization (failure to increase the capillary vascular bed surface available for gas transport by angiogenesis).[2,3] Effective interventions preventing or counteracting established BPD are lacking,[2,4] resulting in stagnant disease incidences despite continuous improvements in neonatal medicine.[5] However, cell-based therapies utilizing exogenous mesenchymal stem- or stromal cells (MSC), a class of immune-evasive mesenchymal progenitor cells[6] obtainable from a variety of tissues,[7,8] showed remarkable lung-protective and lung-regenerative effects in adult lung injury[9-11] and term-born rodent models of arrested lung development, thus sparking hope for an effective treatment of BPD.[12-14] The effects of such cells upon the morphology and development of extremely premature-born lungs, however, remain unclear. Here, we evaluated feasibility, safety, and efficacy of an intravenous cell therapy with human umbilical cord-derived MSC using ventilated baboons receiving two weeks of human-equivalent neonatal intensive care therapy after extremely premature birth with 125 days of gestation (term: 185 days of gestation).

Materials and Methods

Cell Production and Quality Control

Following informed consent of the mother, we isolated MSC from the umbilical cord tissue of a term, healthy infant under current good manufacturing practice (cGMP) conditions based on a protocol we previously described.[15] Briefly, we dissociated the disinfected, mechanically disrupted umbilical cord tissue using DNAse (F. Hoffmann-La Roche), hyaluronidase (Riemser Pharma) and collagenase (Nordmark Arzneimittel) and cultured so-obtained cells for two passages on membrane-based culture systems (Corning) in humidified, hypoxic (5% O_2, 5% CO_2) atmospheres to maintain their potency and avoid onset of cellular senescence during cell production.[16] GMP-compliant Dulbecco's low glucose Modified Eagle Medium (Thermo Fisher) supplemented with 10% platelet-rich plasma[17] was used as culture medium. We froze down the cell product at 8×10^6 cells per mL in 90% human serum albumin, (50 mg/mL solution; Baxter, Deerfield, IL, USA) and 10% dimethyl sulfoxide (WAK-Chemie) in a fixed-rate freezer for storage in the vapor phase of liquid nitrogen.

Characterization of the MSC product (Table 1) as per ISCT consensus criteria[18] was performed using freshly thawed, once-rinsed passage 2 cells prepared in exactly the same way as for injection. Flow cytometry, analyses of colony formation and tri-lineage differentiation potential were performed as previously described.[19] We confirmed immunomodulatory potency of the employed cells by successful induction of indoleamine 2,3-dioxygenase (*IDO*) transcription upon 24 hours of stimulation[20] with 10 ng/mL interferon-γ (R&D Systems), using a validated *IDO* primer assay (QuantiTect, Qiagen). To analyze secretion of stanniocalcin-1 (R&D Systems) and FGF-10 (Abbexa), both suggested to mediate MSC's effects in the (newborn) lung,[3,21,22] we obtained 24-hour, cell-free conditioned medium as described.[19]

Trial Design

The aim of this study was to evaluate feasibility, safety, and efficacy of an intravenous cell therapy with human umbilical cord-derived MSC in extremely premature-born baboons.

Table 1. Characterization and release criteria of the employed umbilical cord tissue-derived mesenchymal stromal cell product.

	Methods	Requirements	Results
Sterility*			
Cultivable bacteria	Blood culture, aerobic, and anaerobic	No growth after 7 days	Sterile
Mycoplasma spp.	Mycoplasma culture	No growth after 14 days	Sterile
Cellular identity: immunophenotype †			
CD73	FACS: clone REA804; APC	>90% positive vs. isotype	99.4% positive
CD90	FACS: clone REA897; FITC	>90% positive vs. isotype	99.0% positive
CD105	FACS: clone REA794; VioBlue	>90% positive vs. isotype	98.0% positive
CD14/CD19/CD34/CD45	FACS: clones REA599, REA675, REA1164 and REA747; PE	< 10% positive vs. isotype	1.90% positive
HLA-DR	FACS: clone REA805; VioGreen	< 10% positive vs. isotype	0.14% positive
Cellular identity: functional characterization †			
Adherence to uncoated plastic surfaces	Seeding on standard cultureware	Adherent cells after 48 h	Confirmed
Morphology	Microscopy of adherent cells	Spindle-shaped, fibroblast-like	Confirmed
Colony formation	Limiting dilution assay	>5 colonies per 1000 cells	19 per 1000 cells
Adipogenic differentiation	Staining: Oil Red O	Stained intracellular lipid droplets in induced cells	Confirmed
	PCR: *FABP4*	>1.5-fold upregulation in induced cells vs. uninduced control	1.7-fold upregulation
Chondrogenic differentiation	Staining: Alcian blue	Stained extracellular glycosamino-glycanes in induced cells	Confirmed
Osteogenic differentiation	Staining: Alizarin red S	Stained extracellular calcium deposits in induced cells	Confirmed
	PCR: *RUNX2*	>1.5-fold upregulation in induced cells vs. uninduced control	4.5-fold upregulation
Cellular potency‡			
Immunomodulation	PCR: *IDO* after stimulation with interferon-γ	$>1 \times 10^3$-fold upregulation vs. unstimulated control	3.78×10^5-fold upregulation
Secretion of stanniocalcin-1	ELISA: R&D Systems DY2958	>0.5 ng stanniocalcin-1/mL	2.0 ng/mL
Secretion of fibroblast growth factor 10 (FGF-10)	ELISA: Abbexa abx251302	>0.5 ng FGF-10/mL	13.7 ng/mL

*Analysed prior to cryopreservation as directed by the European Pharmacopoeia (Ph. Eur.).
†Analysed using freshly thawed, once rinsed passage 2 cells.
‡Analysed using freshly thawed, once rinsed passage 2 cells plated onto plastic cultureware.

We designed the trial based on the assumption that—like in rodents—therapy with MSC improves lung structure in almost every animal.[13] Based on our access to stereology unbiased by design to assess efficacy, we chose "improvement in surface area available for gas exchange vs. placebo" as primary outcome. This outcome is precisely assessable (eg, with a low, describable method-inherent variation $CE_{Stereol.;}$ see below) and dichotomous (e.g., the probability of a purely random experimental outcome equals 0.5). We were therefore able to detect a significant difference at an α-level of 0.05 with as low as $n = 5$ animals per group ($0.5^n = 0.5^5 = 0.03125$) if the parameter changes in the same direction in all animals, thus making the experiment conclusive.[23] However, as the safety of an intravenous MSC therapy in actual premature beings is unclear,[13,24] we included 3 extra animals in the treatment group in case of cell therapy-related deaths or severe adverse events.

Ethics, Husbandry, and Fetal Treatment
Following institutional and external review and approval of the protocol (IACUC-UTHSCSA #20110096AP; USDA protocol #74-R-003; OLAW-NIH #D16-00048), we utilized the 125-day gestational (postmenstrual) age, 14 days ventilated baboon model of extreme prematurity described by Seidner et al.[25] with slight modifications. All procedures involving the premature animals or their mothers were conducted in accordance with the current version of the Animal Welfare Act, the Animal Welfare Regulations and followed the US National Research Council's Guide for the Care and Use of Laboratory Animals and the Public Health Service Policy on Humane Care and Use of Laboratory Animals.

Baboons (*Papio anubis* or *Papio anubis × Papio cynocephalus*) were housed in highly enriched social environments in outside facilities at the Southwest National Primate Research Center. Pregnant animals were subjected to clinical estrous cycle monitoring and ultrasonographic studies at estimated 70 and 100 days of gestation; obtained growth parameters were used to calculate gestational ages. To accelerate fetal lung maturation,[26] we administered two intramuscular doses of 6 mg betamethasone (American Regent) to pregnant animals (Fig. 1A).

Delivery and Support of Transition

Pregnant baboons received general anesthesia and fetuses were delivered by primary caesarean section. Extremely premature-born animals (Table 2) were weighed and placed in plastic wrap to prevent hypothermia. Baboons then received intra-muscular ketamine (10 mg/kg; Putney), Vitamin K (0.5 mg; Hospira). We then intubated the animals orotracheally, using uncuffed endotracheal tubes (Vygon) and slowly instilled 120 mg Poractant alfa (Chiesi Farmaceutici) via the lateral port of the tube. During this procedure, animals were started on pressure-controlled, continuous mandatory ventilation (PC-CMV) with a rate of 40 min^{-1}, peak inspiratory pressure (PIP) of 30 cmH$_2$O, positive end expiratory pressure (PEEP) of 5 cmH$_2$O and a fraction of inspired oxygen (FiO$_2$) of 0.4 utilizing a VIP Gold Bird (CareFusion) respirator. Respiratory support was continuously adapted, based on heart rate and pre-ductal peripheral oxygen saturation (S$_p$O$_2$). A 21 G um-bilical arterial catheter (UAC; Covidien/Medtronic) and a 24 G peripheral inserted central venous catheter (PICC; Vygon) were placed as well as an orogastric tube. The mothers were closely monitored by the attending veterinarian staff after sur-gical repair of incisions and returned to their colonies within 2 to 4 weeks after the surgery.

Clinical Management

Extremely premature-born animals were cared for in humidified, heated incubators (Drägerwerk) as outlined in Fig. 1A. In brief, PC-CMV was continuously adapted to maintain paO$_2$ between 7.3 and 9.3 kPa (55-70 mmHg) and paCO$_2$ between 6.0 and 7.3 kPa (45-55 mmHg). Ketamine and midazolam (Akorn) were provided as required. Heparinized, sodium- and pH-adapted maintenance fluids (normal saline, half-normal saline, or sodium acetate with 1 U/mL unfractionated heparin—all from Hospira) and an in-dividually prepared, amino acid-rich, electrolyte, and glucose-adapted total parenteral nutrition were infused alongside intravenous lipids. Maintenance fluid rates were adapted to maintain mean arterial pressures> >25 mmHg. If hypotensive, a maximum of 2 boluses (10 mL/kg) normal saline was given and escalated to inotropic therapy if required with dopa-mine ± dobutamine (both from Hospira) up to doses of 20 µg/kg/min, respectively. If hypotension persisted, hydrocortisone at 1 mg/kg every 12 hours was initiated and tapered as soon as possible. Acidosis was buffered with sodium bicarbonate (Hospira) at 1 mmol/kg. Animals were transfused with stored placental or maternal packed blood cells at 10 mL/kg if hematocrits persisted below 30%. To prevent sepsis, preemp-tive ampicillin (50 mg/kg), gentamicin (2.5 mg/kg) and van-comycin (15 mg/kg, all from Hospira) were given (Fig. 1A). Whole-body anteroposterior X-ray films were taken every 24 hours to assess the lung, heart, intestines and evaluate the position of the endotracheal tube and the intravascular catheters. Echocardiographic studies were performed daily by a pediatric cardiologist; an open ductus arteriosus was neither treated medically, nor surgically.

Cell Therapy

Right after birth of the animal, we quick-thawed the cell product, rinsed it once in normal saline, strained the suspen-sion through a 40-µm mesh (BD Biosciences) and analyzed cell number and viability automatically (Countess II; Thermo Fisher). The mean of two independent measurements was used. We then injected 10×10^6 umbilical cord tissue-derived MSC per kg birth weight in either 2 mL/kg normal saline over two minutes ($n = 1$, first animal treated) or in a fixed volume of 1.5 mL normal saline ($n = 7$; all other animals) at a rate of 6 mL/hour. Injections were performed via the central ve-nous catheter without an in-line filter device; normal saline (1.5 mL) without cells served as placebo. Animals were ran-domly assigned to receive MSC or placebo.

Physiological Measurements

Arterial blood pressures were continuously obtained from a pressure transducer at the UAC, heart rates by electro-cardiography and S$_p$O$_2$ by pulse oximetry. Ventilation parameters and fluid in- and outputs were recorded hourly, and so-obtained values averaged over 12 hour-intervals for analysis. We obtained arterial blood samples every 4 hours to monitor blood gases, electrolytes and glucose levels utilizing a cartridge-based analysis system (iStat; Abbot). Oxygenation and ventilation indices were calculated as described earlier.[27] Every 48 to 96 hours, a larger (350 µL) blood sample was drawn to obtain a differential blood count and routine blood chemistry (VetScan; Abaxis). If required, we ran fur-ther analyses using the veterinarian laboratory services at the University of Texas Health Center San Antonio.

On day of life seven and again right before necropsy at day of life 14, animals were deeply sedated with ketamine and midazolam and received a single dose of pancuronium bromide (0.1 mg/kg, Hospira) to perform lung function testing using a FlexiVent system (SciReq) as described.[27] In brief, respiratory support was changed from the ventilator to the FlexiVent set to the very same settings the animal was on prior to relaxation. We obtained data on compliance, re-sistance and the total lung capacity using the maneuvers and protocols set by FlexiWare (version 5.3). After completion, the animal was connected back to the ventilator.

Patency of the ductus arteriosus, diameter and shunting direction alongside the flow patterns and peak Doppler velocities across the open ductus and the aortic and pulmo-nary valves were evaluated every 24 hours. The ratio of pul-monary to systemic blood flow Q_p: Q_s as surrogate for the total shunting volume was estimated from the Doppler flow signals obtained across the pulmonary and aortic valves. As all shunting across the open ductus was identified as flowing from the systemic into the pulmonary circulation (left to right), we estimated Q_p indirectly from the flow across the aortic valve, whereas Q_s was obtained by analyzing the flow across the pulmonary valve.

Analysis of Chest Radiographs

Digitalized X-ray films were analyzed to quantify radiographic severity[28,29] of neonatal respiratory distress syndrome (RDS) up to day of life five. RDS was evaluated as grade I if diffuse, fine-granular densities were present; grade II if additional air bronchograms distal of the cardiac shadow were visible; and grade III if, in addition to the features described in grades I and II, the heart and/or diaphragm were partly not differ-entiable from the lung parenchyma. Grade IV was defined as diffuse, bilateral atelectasis radiographically appearing as "white lung". Additionally, lung transparency on day of life 14 was evaluated by grading the transparency of every quad-rant of the thorax image from 0 (no shadowing) over 1 (faint
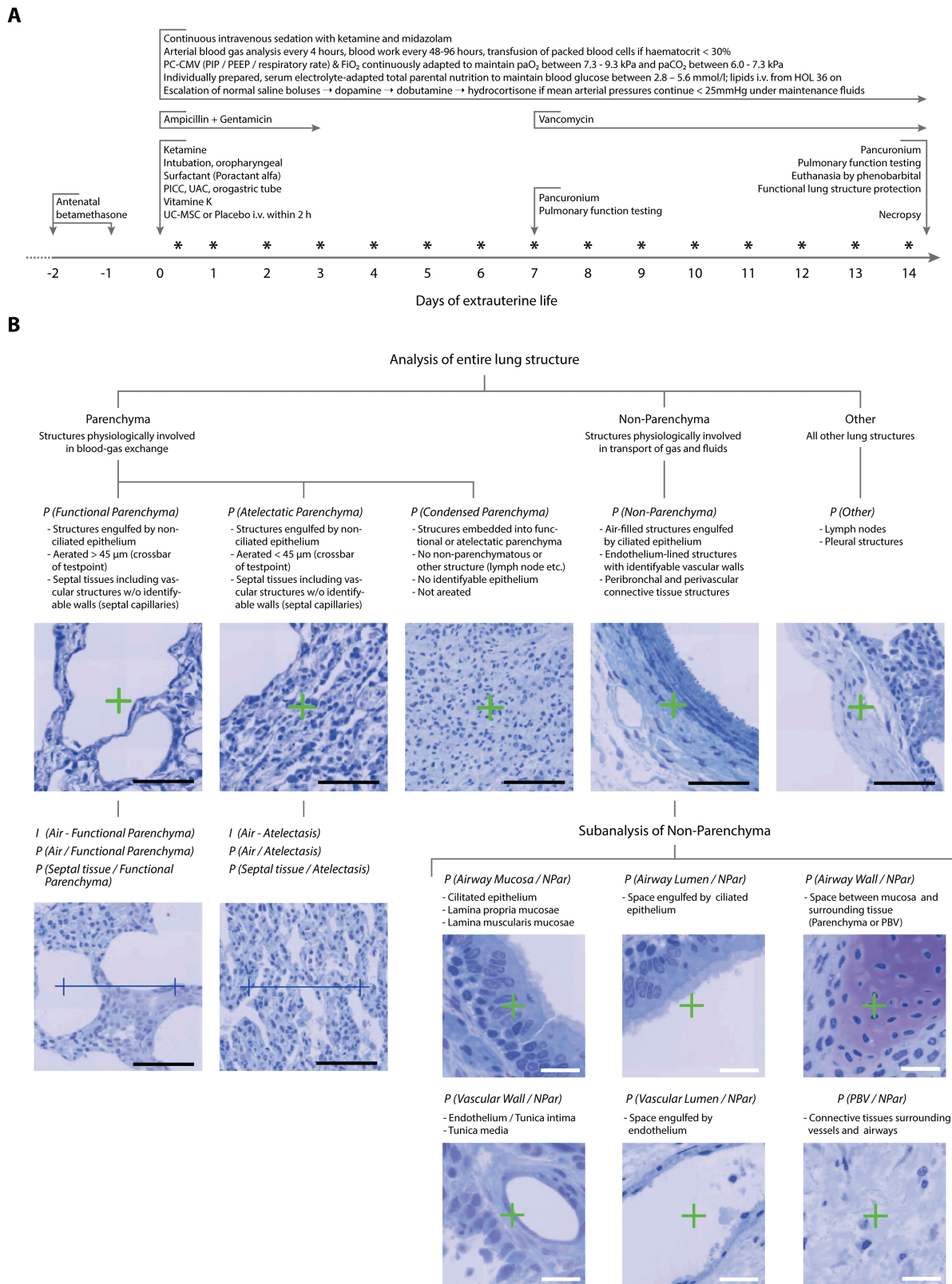
Figure 1. Design of the study. (**A**) Clinical management of extremely premature-born, mechanically ventilated baboons. Abbreviations: FiO$_2$: fraction of inspired oxygen; HOL: hour of life; paO$_2$/paCO$_2$: partial pressures of oxygen/carbon dioxide in the arterial blood; PC-CMV: pressure-controlled continuous mandatory ventilation; PEEP: positive end-expiratory pressure; PICC: peripheral inserted central venous catheter; PIP: positive inspiratory pressure; UAC: umbilical arterial catheter. UC-MSC: umbilical cord tissue-derived mesenchymal stromal cells. Asterisks (*) indicate timepoints of echocardiographic studies. (**B**) Sequential deconstruction of lung tissue into unambiguously identifiable structures. Counting of lung-testsystem interactions (points: *P* and intersections: *I*) enabled quantification of absolute and relative volumes, surfaces and thicknesses unbiased by design. PBV: peribronchial/perivascular connective tissue. Analyses and acquisition of reference volumes was performed at magnifications of 10 × 10 (entire lung structure) or 40 × 10 (subanalysis of non-parenchymatous tissues). Black scale bars: 100μm, white scale bars: 25μm. Staining toluidine blue on Technovit 7100.

Table 2. Baseline characteristics of animals receiving placebo or cell therapy with umbilical cord tissue-derived mesenchymal stromal cells (UC-MSC).

	Placebo (*n* = 5)	UC-MSC (*n* = 8)
Phenotypical characteristics: no. (%)		
Papio anubis × *Papio cynocephalus*	3 (60)	5 (63)
Female	3 (60)	5 (63)
Singletons	5 (100)	8 (100)
Perinatal characteristics: no. (%)		
Complicated pregnancy course*	0 (0)	0 (0)
Complete RDS-prophylaxis	5 (100)	7 (88)
Perinatal characteristics: mean (range)		
Gestational age at birth [day]	126 (125-127)	126 (124-128)
Birth weight [g]	367 (326-386)	372 (332-404)
Baseline vital parameters: mean (CI$_{95\%}$)†		
SpO$_2$ [%]	91 (86-97)	92 (89-96)
FiO$_2$	0.40 (0.21-0.64)	0.29 (0.21-0.37)
Mean airway pressure [cmH$_2$O]	12.0 (11.8-12.2)	11.6 (11.1-12.1)
Mean arterial blood pressure [mmHg]	36 (35-37)	31 (25-37)
Heart rate [min^{-1}]	169 (160-178)	171 (158-184)

*Infections, gestational diabetes, vaginal bleeding, or discordant growth of the fetus.
†Averaged over 60 minutes prior to administration of MSC or placebo. No significant (*P* < .05) differences between groups for any of the parameters by Fisher's exact or Welch's unequal variance *t*-test. Abbreviations: RDS, respiratory distress syndrome; CI$_{95\%}$, 95% confidence interval of the mean; SpO$_2$, peripheral oxygen saturation; FiO$_2$, fraction of inspired oxygen.

shadowing) and 2 (distinct shadowing) to 3 (white lung) and summing up the four individual scores for every quadrant. All radiographic analyses were performed twice in a blinded way. In case of a discrepancy between the first and the second evaluation, and the worse of the two evaluations was used.

Preservation of Functional Lung Structure, Unbiased Sampling

After confirmed cardiocirculatory arrest of the animal, ventilation was continued on unchanged settings while F$_i$O$_2$ was gradually reduced to 0.21. A second endotracheal tube was inserted and gas-tightly secured via a tracheotomy while the orotracheal tube was retracted. After 2 minutes of further ventilation on unchanged settings, the ventilator was switched off at a PEEP of 10 cmH$_2$O in expiration. Following thoracotomy and removal of the heart-lung package with the clamped tube in place, a continuous positive airway pressure (CPAP) of 10 cmH$_2$O was applied via a bubble-CPAP valve (BB Medical Technologies). The right bronchus was tied off, the right lung removed and cut into 25-35 small pieces, which were snap-frozen in liquid nitrogen for subsequent unbiased sampling and analysis of cell engraftment and matrix composition. The right upper lobe

was fixed by inflation with 10% neutral buffered formalin (Thermo Fisher) at a constant pressure of 20 cmH$_2$O for 15 minutes. After embedding in paraffin, 5 µm sections were stained with hematoxylin and eosin.

To prepare lungs for unbiased stereology,[30-33] we advanced an 18 gauge peripheral venous catheter (B. Braun Melsungen) through an insertion in the truncus pulmonalis communis until the tip was perceptible distally of the ductus arteriosus. A ligation between the ductus arteriosus and the tip of the catheter and opening of the left atrium with an incision concluded the cannulation. We then perfused the left lung, while still on CPAP, with a mixture of 1.5% glutaraldehyde and 1.5% paraformaldehyde in 0.15 mol/L HEPES (all from Merck) at pH 7.35 with a pressure of 30 cmH$_2$O for 15 minutes. Subsequently, the trachea was tied off, the endotracheal tube was retracted and the lung fixed for at least two further weeks in the very same fixative at 4 °C.

We then measured the volume V_{Lung} by fluid displacement,[34] using the mean of three independent measurements and obtained 8 to 16 lung pieces of ~0.5 cm^3 using a smooth fractionator-based, systematic-uniformly-randomized (SUR) sampling approach.[31] Required random decisions were made based on coin flips (for dichotomous decisions) or a random number generator relying on atmospheric noise (Randomness and Integrity Services). Following post-fixation with osmium tetroxide and uranyl acetate to avoid shrinking processes interfering with morphometry results,[30,35] tissues were embedded in glycol methacrylate (Technovit 7100; Heraeus-Kulzer). Semi-thin (1.5 µm), isotropic-uniformly-randomized (IUR) sections of the systematic-uniformly-randomized sampled (SURS) blocks were prepared. After staining with toluidine blue, slides were digitalized using an automated scanning microscope (ZEISS Mikroskopie).

Lung Morphometry by Stereology

To investigate the structure of the lungs in an unbiased, blinded and quantitative manner,[30,36] we utilized design-based, computer-assisted stereology (newCAST/Visiopharm). Following mathematically validated analysis methods,[23,30,37] a combined test-system consisting of lines and crosses was projected over randomly orientated, SUR-sampled fields of view obtained from IUR-SURS tissue sections. We counted the number of points hitting the lung structures of interest or the number of intersections of test lines with the surface of gas-exchanging structures with predefined structural cut-offs (Fig. 1B). Following previously described calculation pathways,[30-32,37] we then obtained volume fractions, surface fractions, absolute volumes and surface areas of structures per lung and as well as mean septal thicknesses.

To assess the contribution of biological variation to the observed overall variation,[37] we calculated the coefficient of error of the stereological analysis CE$_{stereol}$ describing the analysis-inherent noise[30] for every animal and parameter as reported.[38]

To obtain information on the spatial distribution of a structural feature within a single animal, we next separated the set of k SURS (fields of view) per animal in m = 25 systematic, uniform subsamples of 8-15 SURS each. We then calculated the parameter estimates $\widehat{R}_{Sub.}$ for every subsample 1 ... m as described[30,31,37] and obtained the sample variance $s^2(\widehat{R}_{Sub.})$ for every parameter and animal as per

$$s^2(\widehat{R}_{\text{Sub.}}) = \frac{1}{m-1} \times \sum_{i=1}^{m} \left(\widehat{R}_{\text{Sub.; } i} - \overline{R}_{\text{Sub.}}\right)^2$$

with $\overline{R}_{\text{Sub.}}$ being the arithmetic mean of $\widehat{R}_{\text{Sub.; } 1...m}$ We then calculated the coefficients of variance for every parameter estimate and animal as per

$$CV(\widehat{R}_{\text{Sub.}}) = \frac{\sqrt{s^2(\widehat{R}_{\text{Sub.}})}}{\overline{R}_{\text{Sub.}}}$$

Thus, $CV(\widehat{R}_{\text{Sub.}})$ describes the bandwidth of spatial distribution of a structural feature/ parameter within the individual organ and represents a surrogate parameter expressing its heterogeneity.

Lung Water Content and Lung Matrix Composition

Three SUR-sampled pieces of right lung tissue per animal were weighed before and after 24 hours of drying at 58 °C to calculate the wet-to-dry ratio as surrogate for the lung water content. We next quantified elastin in these dried samples by quantitative dye-binding methods (Biocolor Life Sciences). The amount of sulfated glycosaminoglycans (sGAG) was investigated using three further SURS lung pieces of approximately 10 mg wet each as directed by the manufacturer (Biocolor Life Sciences). Collagen content was measured indirectly by analyzing hydroxyproline (Merck) in three further uniform-randomized sampled lung pieces of 10 mg wet weight each. Concentrations of collagen were calculated after correcting for the hydroxyproline content of elastin.[39]

Analysis of Cell Engraftment

We searched for the short tandem repeat (STR)-signature of the employed cell product within isolated baboon DNA. Three SUR-sampled pieces of lung, liver, and spleen tissue per animal were obtained prior to isolation of genomic DNA using column-based techniques (Qiagen) and pooling of equal amounts DNA per animal. The same procedure was performed for frozen arterial blood pellets obtained during, and 24 or 72 hours after cell therapy and the administered cell product. We then ran 100 ng genomic DNA per animal and sample using a highly sensitive, 17 loci-extended forensic STR analysis kit (AmpFLSTR NGM SElect) on an Applied Biosystems 3500 forensic genetic analyzer. Data was analyzed utilizing the GeneMapper ID-X software package (all from Thermo Fisher). The STR-pattern of the employed cell product, as well as baboon-specific STR were identified and separated from the signatures of other human DNA (laboratory, medical and veterinarian staff) contaminating the samples.

Statistics

All data were analyzed and visualized using R.[40] Testing for outliers was performed on all data; no outliers were identified and all available data is analyzed, presented and discussed. Event frequencies were compared using Fisher's exact test. Ratio-scaled data was pre-tested for normality using a Shapiro-Wilk test and then compared using either Welch's two-sided, unequal variance *t*-test for normally, or a two-sided Mann-Whitney-*U*-test for not normally distributed data. For multiple comparisons, adjusted levels of significance were calculated using Šidák's correction procedure with an overall type I-error probability of $\alpha = 0.05$. To visualize ratio-scaled data, *t*-distributed 95% confidence intervals of the means were calculated.

Results

Administration of MSC Is Safe and Feasible in Extremely Premature-Born Primates

Preparation of freshly thawed, once-rinsed UC-MSC per kilogram was fast (<30 minutes from start of thawing process to injection-ready cell suspension) and feasible. We recorded a mean viability of 95% (range: 93% to 97%) in the single-cell suspension immediately before injection.

Cardiorespiratory deterioration and subsequent renal failure were observed in the very first animal receiving cells as manual, central venous push of the entire dose UC-MSC in 2 mL normal saline/kg over 2 minutes (Supplementary Fig. S1), leading to an adaption of the protocol and exclusion of this animal from further analyses. In all other animals receiving the dose of 10×10^6 UC-MSC/kg as slow infusion in 4 mL/kg normal saline (mean; range 3.7-4.5 mL/kg) over 15 minutes via the central venous line, no acute adverse reactions—particularly none pointing towards anaphylaxis or pulmonary embolism—were observed (Fig. 2A-D). None of the adverse events noted during subsequent neonatal critical care were specifically attributable to prior administration of UC-MSC (Table 3). In particular, no signs of emerging kidney failure were seen (Fig. 2E-I and Supplementary Fig. S2). Forensic STR analyses confirmed absence of exogenous MSC in unbiased lung, liver and spleen tissue samples 14 days after injection (Fig. 2J-L) while the signature of injected cells was unambiguously identifiable in arterial blood drawn during (intravenous) infusion of the cell product, but not after 24 or 72 hours.

Administration of MSC Is Linked to Improved Cardiovascular Stability

We noted that while ventilation parameters and ductus arteriosus patency did not differ, significantly fewer amounts of fluids and drugs to maintain mean arterial blood pressures ≥ 25 mmHg were required in animals receiving UC-MSC as compared to those being given placebo (Fig. 3A-D and Supplementary Fig. S3A-C). Particularly the need for inotropic medication (dopamine/ dobutamine) was effectively reduced by cell therapy.

No Effects of Exogenous MSC in Extremely Premature-Born, Ventilated Lungs

Administration of UC-MSC had no impact upon the incidence and radiographic severity of neonatal respiratory distress syndrome and was not associated with alterations in radiographic lung structure on day of life 14 (Fig. 4A,B and Supplementary Fig. S4). Injection of cells had no beneficial effect upon compliance or total lung capacity on day of life 14 (Fig. 4C, D), and as compared to placebo, airway resistances trended even higher in the treated group—albeit not reaching levels of significance (Fig. 4E).

Following protection of functional lung structure by intravascular fixation on CPAP, systematic deconstruction of lung structure using stereology led to identification of previously undescribed[41] cell-rich, "condensed" parts in the
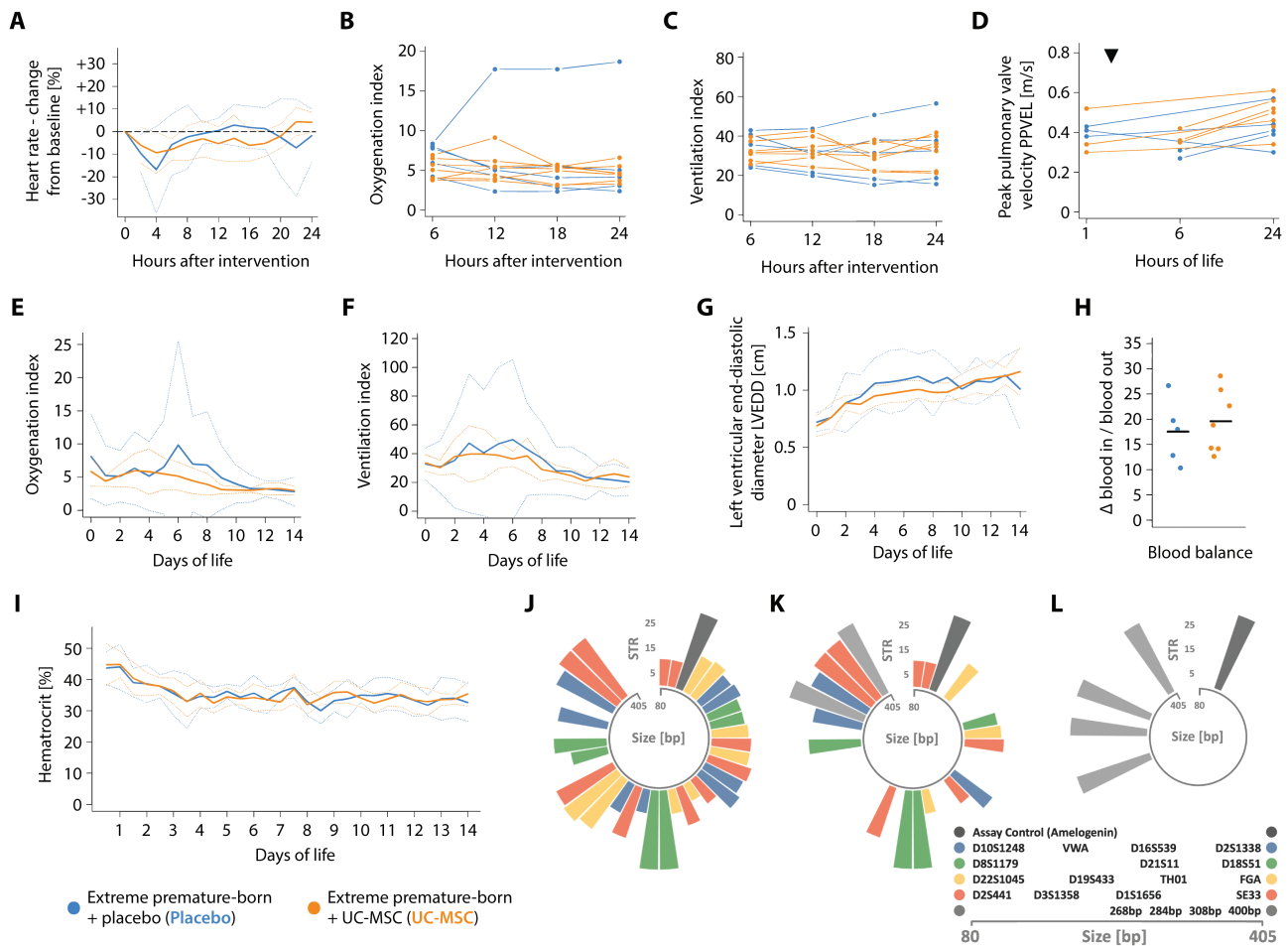
Figure 2. Controlled administration of MSC is safe in critically ill, extremely premature-born baboons. Progression of the (**A**) heart rate, (**B**) oxygenation index, (**C**) ventilation index and the (**D**) peak pulmonary valve velocity (PPVEL) after administration of UC-MSC or placebo, respectively. PPVEL integrates pulmonary perfusion and pulmonary arterial pressure and is expected to drop in cases of substantial changes in pulmonary vascular resistance or right ventricular function (eg, in cases of significant pulmonary arterial obstructions due to the intravenously administered cells). Every graph/ line in (**B-D**) represents data from one animal; data is presented as averaged over 120 minutes (**A**) or six hours (B, C). Echocardiographic studies depicted in (D) were either performed prior to (three animals receiving placebo, three UC-MSC) or four hours after the intervention (two animals receiving placebo, three UC-MSC) and again after 24 hours of life in all animals. The timepoint of intervention is indicated with a triangle (▼). See Supplementary Fig. S1 for information on the clinical course and progression of adverse events in a single extremely premature-born baboon receiving UC-MSC over two minutes and Supplementary Fig. S2 for information on the renal function of the investigated animals. Progression of (**E**) the oxygenation and (**F**) the ventilation index over 2 weeks of neonatal critical care, depicted as group means (solid curves) and 95% confidence interval of the means (dotted curves), averaged over 24-hour intervals. (**G**) Progression of the left ventricular end-diastolic diameter (LVEDD), an estimator of ventricular volume in situations with active left-to-right shunting through an open ductus arteriosus. Data is also depicted as group mean with $CI_{95\%}$. The first echocardiographic study was performed between the first and sixth hour of life (timepoint zero), thereafter every day. (**H**) Blood balance (ie, the difference between transfused and withdrawn blood volumes) on day of life 14, summed up over the entire course of neonatal intensive care. Horizontal bars indicate group means. (**I**) Temporal progression of the hematocrit during neonatal critical care, averaged over 12-hour intervals. No significant ($P < .05$) differences between groups by Mann-Whitney-*U* (H) or Welch's two-sided, unequal variance *t*-test with test level adjustment using Šidák's correction, comparing data for every timepoint (A-G, I). Circular barplots (**J-L**) depicting size (in base pairs—bp—on the circular *x*-axis) and number of short tandem repeats (*y*-axis) on each allele of investigated short tandem repeat (STR)-loci. Equally coloured bars of comparable transcript size indicate the two alleles of an STR-locus, the single dark-grey bar the assay control (amelogenin) and the light-grey bars the four baboon-specific, constant amplificates. STR signature of (J) the employed cell product and (K) an arterial blood sample drawn after approximately one third of the cell dose was given intravenously (positive control). (L) Representative result of an STR analysis of blood drawn 24 hours (*n* = 7) or 72 hours (*n* = 7) after cell administration; or of systematic—uniform sampled pieces of spleen (*n* = 4), liver (*n* = 4), or lung (*n* = 7) obtained on day of life 14 after cell administration. All samples were analysed individually, and 2-4 of the baboon-specific, constant amplificates (light grey) were found per sample and animal besides the assay control (dark grey). Moreover, several human STR-patterns not matching the pattern of the injected cell product were detected in samples and tracked down to the researchers performing the necropsies (not shown).

non-functional parenchyma of the ventilated lungs that—in contrast to atelectatic areas—showed no signs of aeration, no identifiable epithelial structures and were not inflatable with liquid fixatives (Figs. 1B and 4F, Supplementary Fig. S5). These rather rare structures (mean 8.31% of the entire lung volume; confidence interval of the mean $CI_{95\%}$ 4.46%

to 12.16%) were distributed throughout the lungs of all animals, regardless the treatment.

Blinded stereological quantification of lung structure revealed no significant differences between groups; particularly, the alveolar surfaces available for gas exchange, the volumes of functional parenchyma in the lungs and the mean septal

Table 3. Severe adverse events and adverse events during neonatal intensive care.

	Placebo (*n* = 5)		UC- MSC (*n* = 7)	
	Events: no.	Animals: no. (%)	Events: no.	Animals: no. (%)
Any severe adverse event	1	1 (20)	3	2 (29)
Any non-severe adverse event	31	5 (100)	34	7 (100)
Mean events per animal		6.4		5.3
Severe adverse events				
Death	0	0	0	0
Cardiopulmonary resuscitation	0	0	1	1 (14)
Pulmonary hemorrhage	1	1 (20)	2	2 (29)
Adverse events[*]				
Acidosis, severe	1	1 (20)	3	3 (43)
Arrhythmia	1	1 (20)	0	0
Hyperbilirubinemia	1	1 (20)	0	0
Hyperglycemia	0	0	1	1 (14)
Hyperkalemia	1	1 (20)	1	1 (14)
Hypernatremia	0	0	1	1 (14)
Hypoglycemia, severe	3	3 (60)	3	3 (43)
Hypokalemia	4	3 (60)	5	3 (43)
Hyponatremia	4	4 (80)	5	4 (57)
Hypotension requiring at least one catecholamine	4	4 (80)	1	1 (14)
Hypotension requiring hydrocortisone	1	1 (20)	0	0
Macrohematuria	0	0	1	1 (14)
Microhematuria	4	4 (80)	7	7 (100)
Oliguria	4	2 (40)	2	2 (29)
Peripheral arterial occlusion	1	1 (20)	0	0
Positive blood cultures	0	0	1	1 (14)
Proteinuria	1	1 (20)	3	3 (43)
Tachycardia	1	1 (20)	0	0

[*]Events were defined as: acidosis, severe—arterial pH below 7.0 after day of life (DOL)1; hyperbilirubinemia—total bilirubin over 300 μmol/L at any time during the clinical course; hyperglycemia—blood glucose over 11.1 mmol/L; hyperkalemia—potassium over 5.5 mmol/L; hypernatremia—sodium over 150 mmol/L; hypoglycemia, severe—glucose below 1.0 mmol/L after DOL1; hypokalemia—potassium below 3.0 mmol/L; hyponatremia—sodium below 130 mmol/L; proteinuria—moderate or large protein by dipstick in at least two tests within 24 hours, regardless of total proteinuria duration; microhematuria—moderate or large blood by dipstick in at least two tests within 24 hours, regardless of total hematuria duration; Oliguria—less than 0.5 mL/kg/hour for at least 4 hours within a 24-hour period after DOL1; tachycardia—heart rate above 220 beats per minute.
No significant (*P* < .05) differences in overall event frequency or frequency of any specific adverse event were detected by Fisher's exact test.

thickness did not differ with prior administration of UC-MSC (Fig. 4G-I). To further validate these findings, we calculated the analysis-inherent coefficients of error $CE_{Stereol.}$, confirming precise stereological measurements with $CV_{Biol.} > 90\%$ (Supplementary Table S1).

Using subsampling techniques to quantify the spatial distribution of structural features, we detected no impact of cell therapy on prematurity-inherent heterogeneity of lung structure (Supplementary Fig. S6). No significant changes in lung water content or lung matrix composition were noted after cell administration in unbiased samples of lung tissue (Fig. 4K-M), and stereological parameters indicative of early remodeling of airways and pulmonary arteries—pathologies linked to poor long-term outcome of BPD[2,42,43]—were not altered two weeks after UC-MSC infusion (Fig. 4N-O, Supplementary Fig. S7).

Discussion

Here, we report the rather surprising finding that exogenous, systemically administered umbilical cord tissue-derived mesenchymal stromal cells do not ameliorate arrested lung development in extremely premature-born, ventilated baboons. Albeit being safe and leading to a significant cardiocirculatory stabilization of the critically ill animals, no improvements in lung function, lung matrix composition or lung structure were noted 14 days after cell therapy. These findings are in stark contrast to previous data showing that exogenous MSC from various sources—including the umbilical cord tissue—effectively prevent and rescue the hyperoxia-induced arrest of lung development in term-born rodent models of BPD.[13,44-46] We therefore asked whether we have tested the right drug, given at the right dose and the right time via the right route to the right patient[47] and analyzed the obtained data using the right methods.

Drug

Our decision to use UC-MSC was based on the superior availability of the cells, enabling the generation of young, minimally expanded MSC not only for research, but also for further clinical applications.[14,48] UC-MSC have been demonstrated to outperform MSC from other sources in
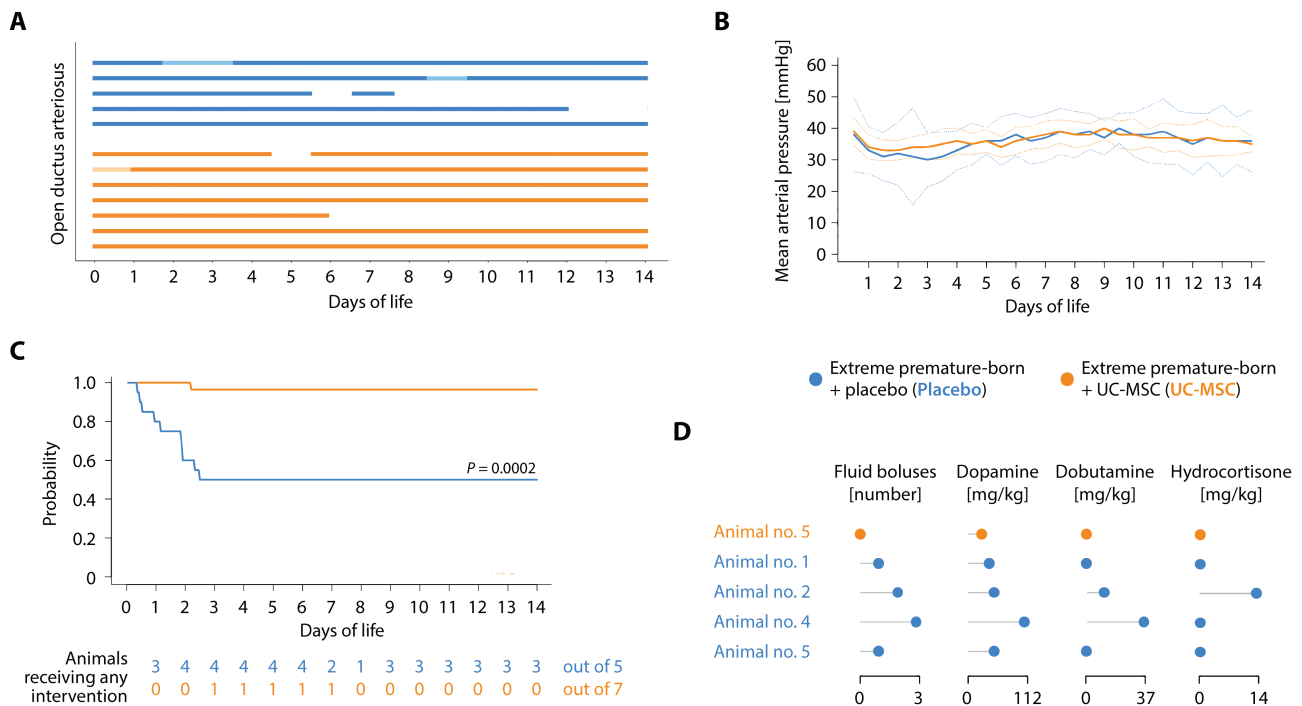
Figure 3. Umbilical cord tissue-derived mesenchymal stromal cells benefit cardiovascular stability in critically ill, extremely premature-born baboons. (**A**) Presence of an open ductus arteriosus, assessed by daily echocardiography. Every bar represents an animal; solid lines an open, gaps a closed ductus arteriosus. Opaque parts indicate days where the ductus was not assessable by echocardiography. All observed shunting occurred from the systemic into the pulmonal circulation (left-to-right). No significant differences between groups, comparing data for every 24-hour interval. (**B**) Temporal progression of the mean arterial pressure, depicted as group mean (solid curves) with 95% confidence interval of the mean ($CI_{95\%}$; dotted curves). No significant differences between groups, comparing data for every twelve-hour interval. (**C**) Event probability for continuing the experiment without requiring escalating interventions (normal saline bolus, dopamine, dobutamine, hydrocortisone) to maintain mean arterial blood pressures ≥ 25 mmHg. Only the start of a new intervention was defined as event; event frequencies were compared on day of life 14. (**D**) Cumulative doses of medications in animals requiring interventions for cardiovascular insufficiency. Every row in the lollipop chart represents one animal. See Supplementary Fig. S3 for further information on the volume status of the animals. All data derives from five placebo and seven MSC-treated animals. Statistics: Event frequencies in (A) and (C) were compared using Fisher's exact method. Welch's two-sided, unequal variance t-test followed by multiple testing adjustment using Šidák's correction was used to compare data presented in (B).

terms of their anti-inflammatory[48,49] and pro-angiogenic[50] potential, making them the (theoretical) optimal cell therapy for diseases suspected to be driven by inflammation and arrested vascularization like BPD.[2,14,51] Here, we used a clinical-grade, passage 2, hypoxia-expanded[16] umbilical cord tissue-derived MSC product manufactured in accordance with current good manufacturing practice (cGMP) conditions to mimic an eventual clinical application as closely as anyhow possible. Besides quality and potency controls required by regulatory agencies, we performed additional investigations confirming extensive secretion of FGF-10 and STC-1 factors linked to the beneficial effects of MSC in rodent models of (neonatal) lung injury.[19,21,22] Moreover, UC-MSC obtained using the very same (but not cGMP-certified) protocol have been shown to effectively reduce mortality and bacterial load in a murine model of neonatal sepsis;[15] rescued arrested lung development in hyperoxia-exposed rodents;[44] and produced extracellular vesicles protecting the lungs and brains of newborn rats,[52] thus demonstrating their overall therapeutic capacity in neonatal organisms. We used freshly-thawed, once-rinsed cell suspensions to mimic an eventual clinical administration of the cells without sub-culturing processes as closely as possible[14,53] and show that—contrasting previous clinical reports[54]—viability of the cells was not compromised by this preparation process. UC-MSC from only one batch/one donor were used to eliminate the impact of batch-to-batch

variability on our experiments. Together, we concluded that the cell product we tested in here harbors the quality, in vitro potency and (term-born rodent model-tested) in vivo efficacy to ameliorate arrested alveolarization. Whether administration of cell-free, MSC-derived drug preparations like conditioned medium[55] or exosomes[52,56] would lead to different effects in extremely premature-born organisms is unclear.

Dose

Most studies using MSC for arrested lung development in neonatal rodents used fixed doses and do not report or normalize to actual birth or body weights.[13] Estimations of cell doses from average birth weights revealed single, intravenously applied doses ranging from 3×10^6 to 1×10^8 MSC/kg in published laboratory studies.[47] Clinical data, however, suggests safety of individual intravenous cell doses up to 10×10^6 MSC/kg in critically ill, adult patients.[54,57] We therefore chose the maximum dose with sound clinical safety evidence and demonstrate that at 10×10^6 MSC/kg, first putative cell-related adverse events (cardiorespiratory deterioration, renal failure) occurred in extremely premature-born animals when this dose was given too fast. We concluded that the dose we administered was appropriate to cause a clinical impact and within the range at which pulmonary effects were seen in rodent models of arrested lung development.
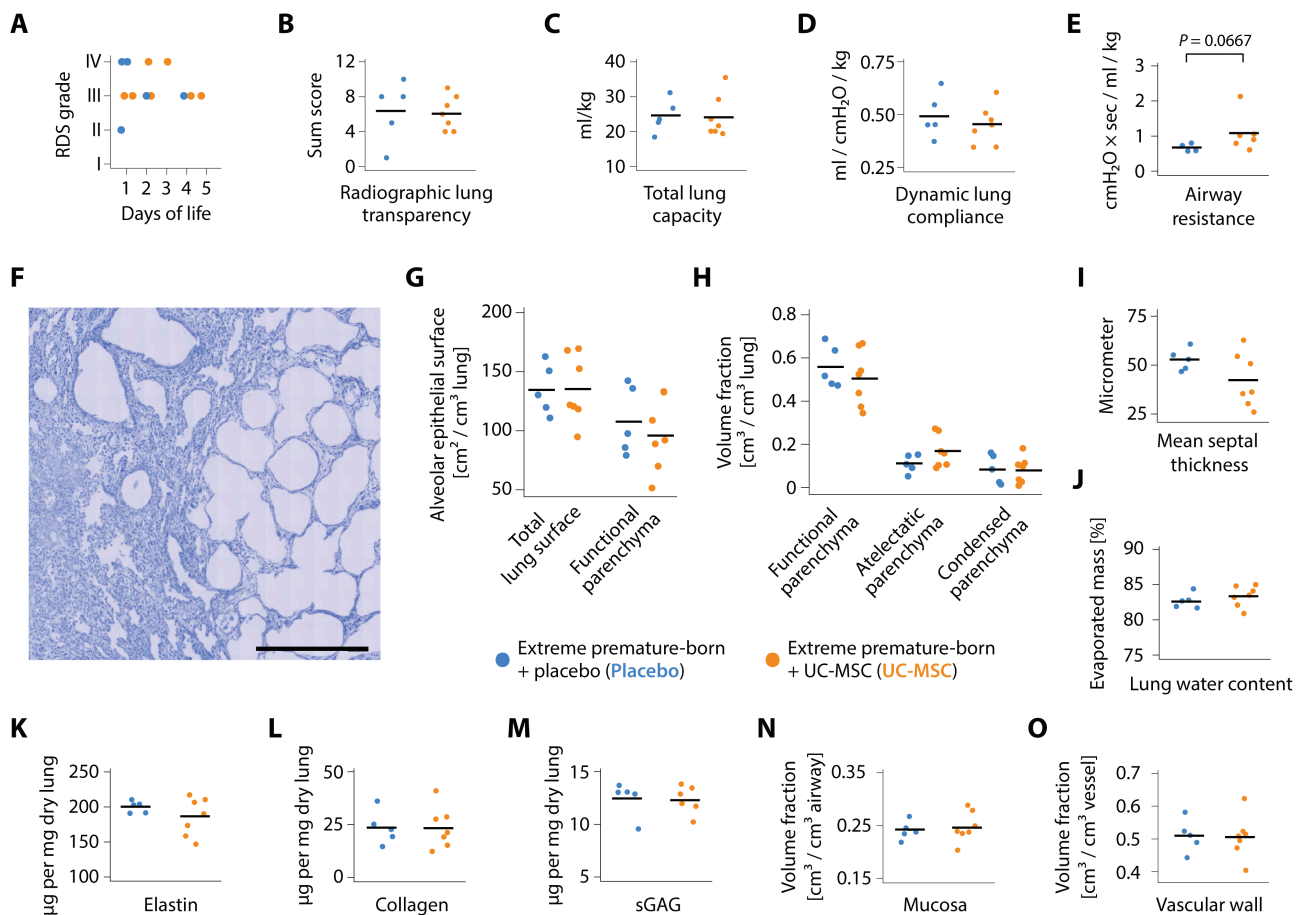
Figure 4. No pulmonary effects of exogenous MSC in extremely premature-born, ventilated baboons. (**A**) Maximum stage of neonatal respiratory distress syndrome (RDS) in the first five days of life and (**B**) lung transparency sum scores on day of life 14. All animals had radiographic signs of RDS from birth on; see Supplementary Fig. S4 for representative baboon chest X-ray films. Datapoints represent results from two individual, blinded image analyses per animal. (**C**) Total lung capacity, (**D**) dynamic lung compliance and (**E**) airway resistance after 14 days of mechanical ventilation. (**F**) Low-magnification photomicrograph showcasing the heterogenous pulmonary architecture an extremely premature-born, 14-day ventilated baboon lung with a side-by-side of atelectatic and emphysematous lung areas. Scale bar = 500 μm. Staining with toluidine blue on 1.5 μm semi-thin Technovit 7100 sections. Also refer to Supplementary Fig. S5. Results of unbiased stereological analyses of the pulmonary structure: (**G**) Total alveolar epithelial surfaces in the functional and atelectatic parenchyma (total lung surface) as well as in the functional parenchyma only; (**H**) volume fractions of functional, atelectatic and condensed parenchyma, and (**I**) mean septal thickness in the functional parenchyma in the lungs of extremely premature-born, ventilated non-human primates 14 days after injection of UC-MSC or placebo. Every datapoint represents mean results of 9-16 (range) isotropic uniformly-randomized, systematic uniformly randomized-sampled pieces of lung tissue (IUR-SURS) per animal; 270 ± 41 (mean ± standard deviation) systematic, uniformly-randomized (SUR) sampled fields of view were analyzed per lung. Refer to Supplementary Fig. S6 and Table S1 for results of further stereological analyses. (**J**) Analysis of lung water content. Every datapoint represents the mean evaporated mass from of three individual SUR-sampled lung pieces per animal. Quantification of the pulmonary extracellular matrix components (**K**) elastin, (**L**) collagen and (**M**) sulphated glycosaminoglycans (sGAG), expressed as μg per mg dried lung tissue. The mean of three individually analysed SUR-sampled lung pieces make one datapoint. Quantification of the (**O**) airway mucosa volume and (**P**) the pulmonary vascular wall volume in relation to the overall vascular or airway volume, respectively. Datapoints represent results from analyses of 622 ± 78 (mean ± standard deviation) SUR-sampled fields of view on 9-16 (range) IUR-SURS per animal. Also see Supplementary Fig. S7. Horizontal bars indicate group means in all graphs and every dot represents data from one animal. No significant ($P < .05$) differences between UC-MSC and placebo-receiving animals for any of the presented data by Welch's 2-sided, unequal variance *t*-test following Shapiro-Wilk testing.

Timing

Available rodent data predominantly derives from studies testing preventive administration of MSC[13] (ie, an administration prior to or during pulmonary injury), albeit increasing evidence for an effective rescue of arrested lung development exists.[44] However, as comparative studies suggested stronger preventive than regenerative effects of MSC,[58] we here administered MSC immediately after birth to protect the extreme premature lung from the arrest of alveolarization.

Route

In term-born rodent models of arrested postnatal lung development, cells are predominantly administered intratracheally;

a first phase II clinical trial also investigated intratracheally administered MSC.[59] However, meta-analyses of rodent-derived data suggest more pronounced pulmonary effects of MSC when administered intravenously.[13] Clinical routine also shows that more and more extremely premature-born infants are not intubated for respiratory support in the delivery room and managed using non-invasive ventilation techniques and less invasive surfactant application strategies,[60,61] making intratracheal administration of MSC via an endotracheal tube in a prospective preventive clinical setting unlikely. We therefore administered the cells intravenously as they directly reach the lungs after injection[62] and are suspected to also exert multiple pleiotropic—in particular neuroprotective—effects.[63]

Patient

The aim of our study was to investigate a single, preventive, intravenous dose of MSC in extremely premature-born organisms. The employed baboon model is perfectly suited for this question as it mimics the significant majority of clinical features of actual human infants at high risk for BPD and—in contrast to any other model—includes extreme premature birth with extreme pulmonary immaturity as *condicio sine qua non* for BPD. However, the model is only representative for extremely premature infants born without inflammatory antecedents, preeclampsia or intrauterine growth restriction, thus excluding a significant proportion of putative BPD patients and calling for carefully designed clinical trials. The same holds true for long-term studies; our experimental protocol allowed only for analyses of immediate to mid-term (up to two weeks) effects, thus making detection of long-term pulmonary effects or the generation of data on survival or exercise capacity after MSC administration not possible.

Analysis

We eventually asked whether we have used the right analysis methodology. As diffuse lung structural changes are a central feature of BPD,[43,64] we aimed at protecting the structural integrity of the lungs during the perfusion fixation process as described above rather than artificially opening up all atelectatic areas by intratracheal inflation with a liquid fixative. We utilized methods to minimize tissue shrinkage, a central problem spoiling morphometric results when using traditional paraffin-based embedding methods,[35] and employed unbiased sampling methods to obtain truly representative material for biochemical and morphometric analyses. Morphometric analyses were performed in a blinded and entirely unbiased manner.[30] Subsequent calculations of stereology-inherent coefficients of error confirmed precise analyses[30,37] using the herein applied stereological evaluation regimen, ruling out inaccurate morphometric analyses as cause for the not detected effect.

Given the widespread use of rather bias-prone morphometric analyses methods[30,36] when evaluating morphological aspects of rodent lung development, the possibility that published improvements in alveolarization and vascularization attributed to MSC administration are to some degree artificial exists and needs to be considered. However, most studies also reported improvements in non-morphometric, physiological parameters like lung function, exercise capacity or survival with MSC therapy, ruling out that reported effects of MSC in rodents are purely anecdotal.

We therefore concluded that albeit giving an optimal cell-based therapeutic to the best available preclinical BPD model using a clinically justifiable dose, time and route and then analyzing lung development using unbiased methods, we were unable to detect any of the beneficial pulmonary effects of MSC seen in term-born rodent models of arrested lung development. The mechanisms of MSC action have been attributed to both, paracrine and direct cell-cell mediated processes, putatively accounting for the pleitropic effect of these cells eventually leading to regeneration of the injured neonatal lung.[47,65] However, the biology behind these processes has so far been investigated in term-born, neonatal rodents only. It is unclear whether an extreme premature-born lung cell disturbed by the extrauterine environment senses and reacts to the signals exerted by an exogenous MSC in the same biological way a term-born lung cell physiologically adapted to extrauterine life does. Importantly, the therapeutic efficacy of exogenous MSC depends on the—in particular inflammatory—microenvironment the cells encounter after administration in vivo.[6,66,67] Whether such a microenvironment exists in extreme premature-born lungs at the time the cells were administered in our study is also unclear.

Our research therefore raises the central question whether exogenous MSC act fundamentally different in term- and preterm-born organisms, warranting investigations on the composition and the cellular dynamics of the extreme premature pulmonary microenvironment in extrauterine conditions. Such investigations would help figuring out whether delayed or repeated MSC administrations to extreme premature-born lungs harbor the potential to prompt effects different than the ones observed here and may have implications on the generalizability of research using term-born animal models to investigate pathologies unique to premature organisms.

We however report several novel secondary results: Using an unbiased systematic approach to deconstruct lungs into unambiguously identifiable structures, we discovered condensed parts of the 14 day-ventilated premature-born pulmonary parenchyma that, to our best knowledge, have not been described so far. In contrast to atelectatic areas or putative artifacts generated during perfusion fixation of aerated lungs, these structures were also present in lung samples fixed by instillation with liquid fixatives. The nature of these structures is elusive. They are detectable in every ventilated animal regardless the treatment, thus ruling out an immune reaction to administered UC-MSC. The structures show no signs of encapsulation or morphology conclusive with abscesses, granuloma, fibrinous-purulent immune cell reaction or fibrosis, are distributed throughout the lungs and show no obvious association to other lung structures like larger airways or intrapulmonary lymph nodes. Further differentiation of the cells in these areas is desirable, but currently hampered by the absence of validated baboon-specific antibodies and relative sparseness of these structures. We speculate that they represent the morphological correlates of alveolitis and collapse induration processes following prolonged (micro) atelectasis, a pathomechanism previously described in the development of adult lung fibrosis.[68,69] How these structures develop in mechanically ventilated extreme premature-born lungs, and whether their progression and/or persistence contributes to the pathogenesis of BPD needs to be investigated.

We also report that a systemic administration of UC-MSC was associated with improved cardiovascular stability of critically ill, extremely premature-born baboons. This is consistent with recent data from genetically engineered MSC in mechanically ventilated sheep;[70] we speculate that this effect of UC-MSC is mediated by an improvement of capillary and vascular integrity as previously described in vitro.[53]

Eventually, we report that MSC—albeit exerting an overall favorable safety profile in non-neonatal patients[57]—harbor the potential to cause systemic side effects if given too fast and/or in a too concentrated manner (here: 5 million MSC/kg/min in 1 mL/kg/min) while not showing such effects when given at 0.6-0.7 million MSC/kg/min in 0.25-0.3 ml/kg/min, generating valuable data for future MSC-based clinical trials.

Conclusions

We provide evidence that a single, systemic administration of UC-MSC right after birth benefits cardiovascular stability,

but neither improves lung structure, nor lung function. This contrast with results gained from term-born animal models of BPD and suggests that exogenous MSC act fundamentally different in term-born and extremely premature-born lungs. Our findings call for further efforts defining the modes of action of exogenous MSC in the extreme premature lung to harness their therapeutic impact while averting potentially deleterious side effects.

Acknowledgments

Funding

Conflict of Interest

Author Contributions

M.A.M., S.R.S., M.R., and **B.T.** conceptualized the research and obtained funding. **S.R.S.** and **M.A.M.** obtained regulatory permissions. **M.A.M., D.F.,** and **N.M.** generated the investigated cell product. Baboon experiments were performed by **M.A.M., S.R.S.,** and **D.C.M.C.** with support from **M.A.H., C.L.B., D.G.A.,** and **L.A.W. D.C.M.C.** performed echocardiographic analyses, **S.B.M.** prepared and blinded the investigated cell product. **I.F.B., L.M., M.A.M.,** and **J.M.** prepared tissues for stereology, which was performed by **M.A.M. J.S.** analyzed X-ray films. Lung matrix analyses were performed by **J.M.** and **L.M.;** forensic short tandem repeat analyses by **S.H. M.A.M.** analyzed the data, drafted the manuscript and prepared the figures. **S.R.S., M.R.,** and **B.T.** supervised the research and revised the manuscript; all authors read and approved the final version of the manuscript.

Data Availability

Digitalized IUR-SURS sections of extremely premature-born, ventilated baboon lungs as well as raw and processed stereological data is available upon request from the corresponding author.

Supplementary Material

Supplementary material is available at *Stem Cells Translational Medicine* online.

References

1. Lawn JE, Kinney M. Preterm birth: now the leading cause of child death worldwide. *Sci Transl Med* 2014;6(263):263ed21; https://dx.doi.org/10.1126/scitranslmed.aaa2563.
2. Thébaud B, Goss KN, Laughon M, et al. Bronchopulmonary dysplasia. *Nat Rev Dis Primers* 2019;5(1):78; https://dx.doi.org/10.1038/s41572-019-0127-7.
3. Lignelli E, Palumbo F, Myti D, et al. Recent advances in our understanding of the mechanisms of lung alveolarization and bronchopulmonary dysplasia. *Am J Physiol Lung Cell Mol Physiol* 2019;317(6):L832–L887; https://dx.doi.org/10.1152/ajplung.00369.2019.
4. Abiramalatha T, Ramaswamy VV, Bandyopadhyay T, et al. Interventions to prevent bronchopulmonary dysplasia in preterm

neonates: an umbrella review of systematic reviews and meta-analyses. *JAMA Pediatr* 2022;176(5):502–516; https://dx.doi.org/10.1001/jamapediatrics.2021.6619.

5. Horbar JD, Edwards EM, Greenberg LT, et al. Variation in performance of neonatal intensive care units in the United States. *JAMA Pediatr* 2017;171(3):e164396; https://dx.doi.org/10.1001/jamapediatrics.2016.4396.

6. Krampera M, Le Blanc K. Mesenchymal stromal cells: putative microenvironmental modulators become cell therapy. *Cell Stem Cell* 2021;28(10):1708–1725; https://dx.doi.org/10.1016/j.stem.2021.09.006.

7. Pittenger MF, Discher DE, Péault BM, et al. Mesenchymal stem cell perspective: cell biology to clinical progress. *NPJ Regen Med* 2019;4:22; https://dx.doi.org/10.1038/s41536-019-0083-6.

8. Soliman H, Theret M, Scott W, et al. Multipotent stromal cells: one name, multiple identities. *Cell Stem Cell* 2021;28(10):1690–1707; https://dx.doi.org/10.1016/j.stem.2021.09.001.

9. Wick KD, Leligdowicz A, Zhuo H, et al. Mesenchymal stromal cells reduce evidence of lung injury in patients with ARDS. *JCI Insight* 2021;6(12):148983; https://dx.doi.org/10.1172/jci.insight.148983.

10. Masterson CH, Ceccato A, Artigas A, et al. Mesenchymal stem/stromal cell-based therapies for severe viral pneumonia: therapeutic potential and challenges. *Intensive Care Med Exp* 2021;9(1):61; https://dx.doi.org/10.1186/s40635-021-00424-5.

11. Kirkham AM, Bailey AJM, Monaghan M, et al. Updated living systematic review and meta-analysis of controlled trials of mesenchymal stromal cells to treat COVID-19: a framework for accelerated synthesis of trial evidence for rapid approval-FASTER approval. *Stem Cells Transl Med* 2022;11(7):675–687; https://dx.doi.org/10.1093/stcltm/szac038.

12. Augustine S, Cheng W, Avey MT, et al. Are all stem cells equal? Systematic review, evidence map, and meta-analyses of preclinical stem cell-based therapies for bronchopulmonary dysplasia. *Stem Cells Transl Med* 2020;9(2):158–168; https://dx.doi.org/10.1002/sctm.19-0193.

13. Augustine S, Avey MT, Harrison B, et al. Mesenchymal stromal cell therapy in bronchopulmonary dysplasia: systematic review and meta-analysis of preclinical studies. *Stem Cells Transl Med* 2017;6(12):2079–2093; https://dx.doi.org/10.1002/sctm.17-0126.

14. Rüdiger M, Kirpalani H, Steinhorn R, et al. How to introduce MSC-based therapy for the developing lung safely into clinical care? *Pediatr Res* 2020;88(3):365–368; https://dx.doi.org/10.1038/s41390-020-0758-0.

15. Zhu Y, Xu L, Collins JJP, et al. Human umbilical cord mesenchymal stromal cells improve survival and bacterial clearance in neonatal sepsis in rats. *Stem Cells Dev* 2017;26(14):1054–1064; https://dx.doi.org/10.1089/scd.2016.0329.

16. Silva LHA, Antunes MA, Dos Santos CC, et al. Strategies to improve the therapeutic effects of mesenchymal stromal cells in respiratory diseases. *Stem Cell Res Ther* 2018;9(1):45; https://dx.doi.org/10.1186/s13287-018-0802-8.

17. von Bonin M, Stölzel F, Goedecke A, et al. Treatment of refractory acute GVHD with third-party MSC expanded in platelet lysate-containing medium. *Bone Marrow Transplant* 2009;43(3):245–251; https://dx.doi.org/10.1038/bmt.2008.316.

18. Dominici M, Le Blanc K, Mueller I, et al. Minimal criteria for defining multipotent mesenchymal stromal cells. The International Society for Cellular Therapy position statement. *Cytotherapy* 2006;8(4):315–317; https://dx.doi.org/10.1080/14653240600855905.

19. Möbius MA, Freund D, Vadivel A, et al. Oxygen disrupts human fetal lung mesenchymal cells. implications for bronchopulmonary dysplasia. *Am J Respir Cell Mol Biol* 2019;60(5):592–600; https://dx.doi.org/10.1165/rcmb.2018-0358OC.

20. François M, Romieu-Mosurez R, Li M, et al. Human MSC suppression correlates with cytokine induction of indoleamine 2,3-dioxygenase and bystander M2 macrophage differentiation. *Mol Ther* 2012;20(1):187–195; https://dx.doi.org/10.1038/mt.2011.189.

21. Chao C-M, Moiseenko A, Kosanovic D, et al. Impact of Fgf10 deficiency on pulmonary vasculature formation in a mouse model of bronchopulmonary dysplasia. *Hum Mol Genet* 2019;28(9):1429–1444; https://dx.doi.org/10.1093/hmg/ddy439.

22. Ono M, Ohkouchi S, Kanehira M, et al. Mesenchymal stem cells correct inappropriate epithelial-mesenchyme relation in pulmonary fibrosis using stanniocalcin-1. *Mol Ther* 2015;23(3):549–560; https://dx.doi.org/10.1038/mt.2014.217.

23. Weibel E, Cruz-Orive L. Morphometric methods. In: Crystal RG, West JB, Weibel ER, Barnes PJ, eds. *The Lung - Scientific Foundations*. 2nd ed. Philadelphia, Pennsylvania, USA: Lippincott Williams & Wilkins; 1997.

24. Pierro M, Thébaud B, Soll R. Mesenchymal stem cells for the prevention and treatment of bronchopulmonary dysplasia in preterm infants. *Cochrane Database Syst Rev* 2017;11:CD011932; https://dx.doi.org/10.1002/14651858.CD011932.pub2.

25. Seidner SR, Jobe AH, Coalson JJ, et al. Abnormal surfactant metabolism and function in preterm ventilated baboons. *Am J Respir Crit Care Med* 1998;158(6):1982–1989; https://dx.doi.org/10.1164/ajrccm.158.6.9804128.

26. McGoldrick E, Stewart F, Parker R, et al. Antenatal corticosteroids for accelerating fetal lung maturation for women at risk of preterm birth. *Cochrane Database of Systematic Reviews* 2020;(12); https://dx.doi.org/10.1002/14651858.CD004454.pub4.

27. McCurnin DC, Pierce RA, Chang LY, et al. Inhaled NO improves early pulmonary function and modifies lung growth and elastin deposition in a baboon model of neonatal chronic lung disease. *Am J Physiol Lung Cell Mol Physiol* 2005;288(3):L450–459; https://dx.doi.org/10.1152/ajplung.00347.2004.

28. Agrons GA, Courtney SE, Stocker JT, et al. From the archives of the AFIP: lung disease in premature neonates: radiologic-pathologic correlation. *Radiographics* 2005;25(4):1047–1073; https://dx.doi.org/10.1148/rg.254055019.

29. Liu J. Respiratory distress syndrome in full-term neonates. *J Neonatal Biol* 2012;S1(01); https://dx.doi.org/10.4172/2167-0897.S1-e001.

30. Hsia CCW, Hyde DM, Ochs M, et al. An official research policy statement of the American Thoracic Society/European Respiratory Society: standards for quantitative assessment of lung structure. *Am J Respir Crit Care Med* 2010;181(4):394–418; https://dx.doi.org/10.1164/rccm.200809-1522ST.

31. Ochs M, Mühlfeld C. Quantitative microscopy of the lung: a problem-based approach. Part 1: basic principles of lung stereology. *Am J Physiol Lung Cell Mol Physiol* 2013;305(1):L15–22; https://dx.doi.org/10.1152/ajplung.00429.2012.

32. Mühlfeld C, Ochs M. Quantitative microscopy of the lung: a problem-based approach. Part 2: stereological parameters and study designs in various diseases of the respiratory tract. *Am J Physiol Lung Cell Mol Physiol* 2013;305(3):L205–221; https://dx.doi.org/10.1152/ajplung.00427.2012.

33. Tschanz S, Schneider JP, Knudsen L. Design-based stereology: planning, volumetry and sampling are crucial steps for a successful study. *Ann Anat* 2014;196(1):3–11; https://dx.doi.org/10.1016/j.aanat.2013.04.011.

34. Scherle W. A simple method for volumetry of organs in quantitative stereology. *Mikroskopie* 1970;26(1):57–60.

35. Schneider JP, Ochs M. Alterations of mouse lung tissue dimensions during processing for morphometry: a comparison of methods. *Am J Physiol Lung Cell Mol Physiol* 2014;306(4):L341–350; https://dx.doi.org/10.1152/ajplung.00329.2013.

36. Weibel ER, Hsia CCW, Ochs M. How much is there really? Why stereology is essential in lung morphometry. *J Appl Physiol* (1985) 2007;102(1):459–467; https://dx.doi.org/10.1152/japplphysiol.00808.2006.

37. Howard CV, Reed MG. *Unbiased Stereology. 20th Anniversary Edition*. Coleraine, UK: QTP Publications; 2018.

38. Cruz-Orive L-M. Best linear unbiased estimators for stereology. *Biometrics* 1980;36(4):595–605; https://dx.doi.org/10.2307/2556113.

39. Stoilov I, Starcher BC, Mecham RP, et al. Measurement of elastin, collagen, and total protein levels in tissues. *Methods Cell Biol* 2018;143:133–146; https://dx.doi.org/10.1016/bs.mcb.2017.08.008.

40. R Core Team. *R: a language and environment for statistical computing*. 2018.

41. Coalson JJ, Winter VT, Siler-Khodr T, et al. Neonatal chronic lung disease in extremely immature baboons. *Am J Respir Crit Care Med* 1999;160(4):1333–1346; https://dx.doi.org/10.1164/ajrccm.160.4.9810071.

42. Mourani PM, Mandell EW, Meier M, et al. Early Pulmonary Vascular Disease in Preterm Infants Is Associated with Late Respiratory Outcomes in Childhood. *Am J Respir Crit Care Med* 2019;199(8):1020–1027; https://dx.doi.org/10.1164/rccm.201803-0428OC.

43. Wu KY, Jensen EA, White AM, et al. Characterization of disease phenotype in very preterm infants with severe bronchopulmonary dysplasia. *Am J Respir Crit Care Med* 2020;201(11):1398–1406; https://dx.doi.org/10.1164/rccm.201907-1342OC.

44. O'Reilly M, Möbius MA, Vadivel A, et al. Late rescue therapy with cord-derived mesenchymal stromal cells for established lung injury in experimental bronchopulmonary dysplasia. *Stem Cells Dev* 2020;29(6):364–371; https://dx.doi.org/10.1089/scd.2019.0116.

45. O'Reilly M, Thébaud B. Animal models of bronchopulmonary dysplasia. The term rat models. *Am J Physiol Lung Cell Mol Physiol* 2014;307(12):L948–958; https://dx.doi.org/10.1152/ajplung.00160.2014.

46. Berger J, Bhandari V. Animal models of bronchopulmonary dysplasia. The term mouse models. *Am J Physiol Lung Cell Mol Physiol* 2014;307(12):L936–947; https://dx.doi.org/10.1152/ajplung.00159.2014.

47. Möbius MA, Thébaud B. Cell therapy for bronchopulmonary dysplasia: promises and perils. *Paediatr Respir Rev* 2016;20:33–41; https://dx.doi.org/10.1016/j.prrv.2016.06.001.

48. Vaka R, Khan S, Ye B, et al. Direct comparison of different therapeutic cell types susceptibility to inflammatory cytokines associated with COVID-19 acute lung injury. *Stem Cell Res Ther* 2022;13(1):20; https://dx.doi.org/10.1186/s13287-021-02699-7.

49. Abdelgawad M, Bakry NS, Farghali AA, et al. Mesenchymal stem cell-based therapy and exosomes in COVID-19: current trends and prospects. *Stem Cell Res Ther* 2021;12(1):469; https://dx.doi.org/10.1186/s13287-021-02542-z.

50. Kehl D, Generali M, Mallone A, et al. Proteomic analysis of human mesenchymal stromal cell secretomes: a systematic comparison of the angiogenic potential. *NPJ Regen Med* 2019;4:8; https://dx.doi.org/10.1038/s41536-019-0070-y.

51. Appuhn SV, Siebert S, Myti D, et al. Capillary changes precede disordered alveolarization in a mouse model of bronchopulmonary dysplasia. *Am J Respir Cell Mol Biol* 2021;65(1):81–91; https://dx.doi.org/10.1165/rcmb.2021-0004OC.

52. Lithopoulos MA, Strueby L, O'Reilly M, et al. Pulmonary and neurologic effects of mesenchymal stromal cell extracellular vesicles in a multifactorial lung injury model. *Am J Respir Crit Care Med* 2022;205(10):1186–1201; https://dx.doi.org/10.1164/rccm.202012-4520OC.

53. Tan Y, Salkhordeh M, Wang J-P, et al. Thawed mesenchymal stem cell product shows comparable immunomodulatory potency to cultured cells in vitro and in polymicrobial septic animals. *Sci Rep* 2019;9(1):18078; https://dx.doi.org/10.1038/s41598-019-54462-x.

54. Matthay MA, Calfee CS, Zhuo H, et al. Treatment with allogeneic mesenchymal stromal cells for moderate to severe acute respiratory distress syndrome (START study): a randomised phase 2a safety trial. *Lancet Respir Med* 2019;7(2):154–162; https://dx.doi.org/10.1016/S2213-2600(18)30418-1.

55. Emukah C, Dittmar E, Naqvi R, et al. Mesenchymal stromal cell conditioned media for lung disease: a systematic review and meta-analysis of preclinical studies. *Respir Res* 2019;20(1):239; https://dx.doi.org/10.1186/s12931-019-1212-x.

56. Willis GR, Reis M, Gheinani AH, et al. Extracellular vesicles protect the neonatal lung from hyperoxic injury through the epigenetic and transcriptomic reprogramming of myeloid cells. *Am J Respir Crit Care Med* 2021;204(12):1418–1432; https://dx.doi.org/10.1164/rccm.202102-0329OC.

57. Thompson M, Mei SHJ, Wolfe D, et al. Cell therapy with intravascular administration of mesenchymal stromal cells continues to appear safe: An updated systematic review and meta-analysis. *EClinicalMedicine* 2020;19:100249; https://dx.doi.org/10.1016/j.eclinm.2019.100249.

58. Chang YS, Choi SJ, Ahn SY, et al. Timing of umbilical cord blood derived mesenchymal stem cells transplantation determines therapeutic efficacy in the neonatal hyperoxic lung injury. *PLoS ONE* 2013;8(1):e52419; https://dx.doi.org/10.1371/journal.pone.0052419.

59. Ahn SY, Chang YS, Lee MH, et al. Stem cells for bronchopulmonary dysplasia in preterm infants: a randomized controlled phase II trial. *Stem Cells Transl Med* 2021;10(8):1129–1137; https://dx.doi.org/10.1002/sctm.20-0330.

60. Madar J, Roehr CC, Ainsworth S, et al. European Resuscitation Council Guidelines 2021: newborn resuscitation and support of transition of infants at birth. *Resuscitation* 2021;161:291–326; https://dx.doi.org/10.1016/j.resuscitation.2021.02.014.

61. Abdel-Latif ME, Davis PG, Wheeler KI, et al. Surfactant therapy via thin catheter in preterm infants with or at risk of respiratory distress syndrome. *Cochrane Database Syst Rev* 2021;5:CD011672; https://dx.doi.org/10.1002/14651858.CD011672.pub2.

62. Weiss DJ, Casaburi R, Flannery R, et al. A placebo-controlled, randomized trial of mesenchymal stem cells in COPD. *Chest* 2013;143(6):1590–1598; https://dx.doi.org/10.1378/chest.12-2094.

63. Archambault J, Moreira A, McDaniel D, et al. Therapeutic potential of mesenchymal stromal cells for hypoxic ischemic encephalopathy: a systematic review and meta-analysis of preclinical studies. *PLoS One* 2017;12(12):e0189895; https://dx.doi.org/10.1371/journal.pone.0189895.

64. Spielberg DR, Walkup LL, Stein JM, et al. Quantitative CT scans of lung parenchymal pathology in premature infants ages 0-6 years. *Pediatr Pulmonol* 2018;53(3):316–323; https://dx.doi.org/10.1002/ppul.23921.

65. Hurskainen M, Cyr-Depauw C, Thébaud B. Insights into the mechanisms of alveolarization - implicastions for lung regeneration and cell therapies. *Semin Fetal Neonatal Med* 2022;27(1):101243; https://dx.doi.org/10.1016/j.siny.2021.101243.

66. Islam D, Huang Y, Fanelli V, et al. Identification and modulation of microenvironment is crucial for effective mesenchymal stromal cell therapy in acute lung injury. *Am J Respir Crit Care Med* 2019;199(10):1214–1224; https://dx.doi.org/10.1164/rccm.201802-0356OC.

67. Dunbar H, Weiss DJ, Rolandsson Enes S, et al. The inflammatory lung microenvironment; a key mediator in MSC licensing. *Cells* 2021;10(11):2982; https://dx.doi.org/10.3390/cells10112982.

68. Burkhardt A. Alveolitis and collapse in the pathogenesis of pulmonary fibrosis. *Am Rev Respir Dis* 1989;140(2):513–524; https://dx.doi.org/10.1164/ajrccm/140.2.513.

69. Knudsen L, Ruppert C, Ochs M. Tissue remodelling in pulmonary fibrosis. *Cell Tissue Res* 2017;367(3):607–626; https://dx.doi.org/10.1007/s00441-016-2543-2.

70. Millar JE, Bartnikowski N, Passmore MR, et al. Combined mesenchymal stromal cell therapy and extracorporeal membrane oxygenation in acute respiratory distress syndrome. a randomized controlled trial in sheep. *Am J Respir Crit Care Med* 2020;202(3):383–392; https://dx.doi.org/10.1164/rccm.201911-2143OC.